remote sensing

MDPI

Article

Distribution of Artisanal and Small-Scale Gold Mining in the Tapajós River Basin (Brazilian Amazon) over the Past 40 Years and Relationship with Water Siltation

Felipe de Lucia Lobo [1,2,*], Maycira Costa [1], Evlyn Márcia Leão de Moraes Novo [2] and Kevin Telmer [1,3]

1 Spectral Lab, Department of Geography, University of Victoria, 3800 Finnerty Road, Victoria, BC V8P 5C2, Canada; maycira@uvic.ca (M.C.); ktelmer@artisanalgold.org (K.T.)
2 Remote Sensing Division, National Institute for Space Research (INPE), Av. dos Astronautas 1758, São José dos Campos, SP 12227-010, Brazil; evlyn.novo@inpe.br
3 Artisanal Gold Council, 101-732 Cormorant St., Victoria, BC V8W 4A5, Canada
* Correspondence: lobo@uvic.ca; Tel.: +55-012-3208-6810

Academic Editors: Petri Pellikka, Lars Eklundh, Richard Gloaguen and Prasad S. Thenkabail
Received: 27 April 2016; Accepted: 5 July 2016; Published: 9 July 2016

Abstract: An innovative remote sensing approach that combines land-use change and water quality information is proposed in order to investigate if Artisanal and Small-scale Gold Mining (ASGM) area extension is associated with water siltation in the Tapajós River Basin (Brazil), containing the largest small-scale gold mining district in the world. Taking advantage of a 40-year period of the multi-satellite imagery archive, the objective of this paper is to build a normalized time-series in order to evaluate the influence of temporal mining expansion on the water siltation data (TSS, Total Suspended Solids concentration) derived from previous research. The methodological approach was set to deliver a full characterization of the ASGM expansion from its initial stages in the early 1970s to the present. First, based on IRS/LISSIII images acquired in 2012, the historical Landsat image database (1973–2001) was corrected for radiometric and atmospheric effects using dark vegetation as reference to create a normalized time-series. Next, a complete update of the mining areas distribution in 2012 derived from the TerraClass Project (an official land-use classification for the Brazilian Amazon) was conducted having IRS/LISSIII as the base map with the support of auxiliary data and vector editing. Once the ASGM in 2012 was quantified (261.7 km^2) and validated with photos, a reverse classification of ASGM in 2001 (171.7 km^2), 1993 (166.3 km^2), 1984 (47.5 km^2), and 1973 (15.4 km^2) with the use of Landsat archives was applied. This procedure relies on the assumption that ASGM changes in the land cover are severe and remain detectable from satellite sensors for decades. The mining expansion area over time was then combined with the (TSS) data retrieved from the same atmospherically corrected satellite imagery based on the literature. In terms of gold mining expansion and water siltation effects, four main periods of ASGM activities were identified in the study area: (i) 1958–1977, first occurrence of mining activities and low water impacts; (ii) 1978–1993, introduction of low-budget mechanization associated with very high gold prices resulting in large mining area expansion and high water siltation levels; (iii) 1994–2003, general recession of ASGM activities and exhaustion of easy-access gold deposits, resulting in decreased TSS; (iv) 2004 to present, intensification of ASGM encouraged by high gold prices, resulting in an increase of TSS.

Keywords: land use change; gold mining; water siltation; time-series analysis; Landsat; IRS/LISSIII

1. Introduction

Artisanal and Small-scale Gold Mining (ASGM) refers to the mining practiced using rudimentary technology by individuals, groups, or communities. This practice is primarily found in developing countries of South America, Asia, and Africa [1–3]. In the Amazon, substantial ASGM activities started in the 1950s at a few sites, called *garimpos*. Currently, hundreds of thousands of people are directly involved in ASGM in the Amazon Basin due to the relatively high rise in the gold price (USD 1100/oz) in recent years [2,4,5]. In Brazil alone, ASGM gold production is responsible for 30 tonnes of gold per year, of which about 26% is produced in the Tapajós River Basin in the Amazon by approximately 50,000 miners (or *garimpeiros*) who are distributed in more than 300 mining sites [4–7].

Despite its contribution to the local economy, ASGM causes several environmental impacts, such as mercury contamination, water siltation, and landscape degradation [2,8]. The ASGM local practice results in high water siltation due to the discharge of sediment from the margins of the rivers, where exploitation of alluvial deposits usually takes place [4]. As the miners exploit a particular area of the alluvial plain, new pits are opened, and the mine tailings (water + sediment) are usually discharged back into the river drainage, or to adjacent small ponds/lakes. The discharge of sediment into the water results in severe impacts on the water quality, such as decreasing light availability for primary production [9], and changing benthic [10] and fish communities [11].

The associated ASGM changes in the landscape (roads, aerial strips) generally include deforestation of the area in order to access gold deposits and settlements. Since several of these settlements are informally operating inside remote protected areas and indigenous lands in the Amazon [5,12], delineation of historical mining areas using satellite images is the only possible tool that allows for better understanding of changes in river water quality associated with gold mining practices in the region. The combined set of information, land use change and water quality change associated with ASGM, is of considerable interest to the land management community for the purposes of evaluation regarding social and environmental implications of gold mining activities in the region. At the same time, it provides information for the proposition of public policies which aim for the recovery of degraded areas and sustainable use of water and mineral resources [5,8,12].

Therefore, with the benefit of the available 40-year period of the Landsat archive, the objective of this paper is to build a normalized imagery time-series in order to extract land use change for four tributaries in the Tapajós River Basin (Jamanxim, Crepori, Tocantinzinho and Novo river basins) and evaluate its influence on the water siltation observed in previous research [12]. To accomplish this, the quality and the time span of the satellite images are of key importance. Studies that aim to detect land use change based on a variation of the target's reflectance requires radiometric and atmospheric correction with further normalization or intercalibration of the satellite images [13,14]. Moreover, detection of environmental changes caused by anthropogenic activities requires data that covers at least the entire period before the initial activities (pristine condition) and up to its present state. In the case of the Tapajós region (the geographic focus of this research), the first gold rush started in the late 1970s after the first Landsat MSS images were acquired (early 1970s). In this context, all historical Landsat archive images (1973–2001) were inter-calibrated with IRS/LISSIII images acquired in 2012, for which atmospheric corrections were previously validated with in situ radiometric measurements [12]. The inter-calibration process used dark vegetation as reference to create a normalized time-series to assure that temporal changes are only due to anthropogenic activities and not to atmospheric or radiometric effects. The corrected Landsat satellite imagery from 1973 (pristine conditions), 1984, 1993, 2001, and 2012 (IRS/LISSIII images) was used as a base map to identify and quantify the ASGM areas. The spatial and temporal effects of ASGM on water siltation (derived from satellite images, [12]) were then conducted based on the land-cover dynamic, general mining techniques, and socio-economic framework throughout the decades.

2. Study Area

The lower section of the Tapajós River Basin covers about 130,370 km^2 and is located at the center of the Brazilian Amazon (Figure 1a). The first occurrence of mining activities started in 1958 and were based on manual efforts, without any mechanization [15]. In 1978, mechanization, such as dredges, was introduced, mostly in the Tapajós and larger tributaries. In the 1980s, exploitation of colluvial ore deposits began with water-jet systems [8] resulting in a boom of the mining population, which reached approximately 150,000 in 1989 [8], with gold production reaching approximately 25 tonnes a year. During this decade, more than 400 airstrips and over 600 mining sites (*garimpos*) were reported [8]. The gold rush in Tapajós compelled the Brazilian government to create the Gold Mining Reserve in 1983, along with other policies, to support local miners and to reduce socio-environmental impacts, with no satisfactory results [5]. In the late 1990s, ASGM decreased drastically, mainly discouraged by the low price of gold and the exhaustion of easy-access alluvial gold deposits. Consequently, gold production reduced gradually to approximately 10 tonnes per year in 2000.

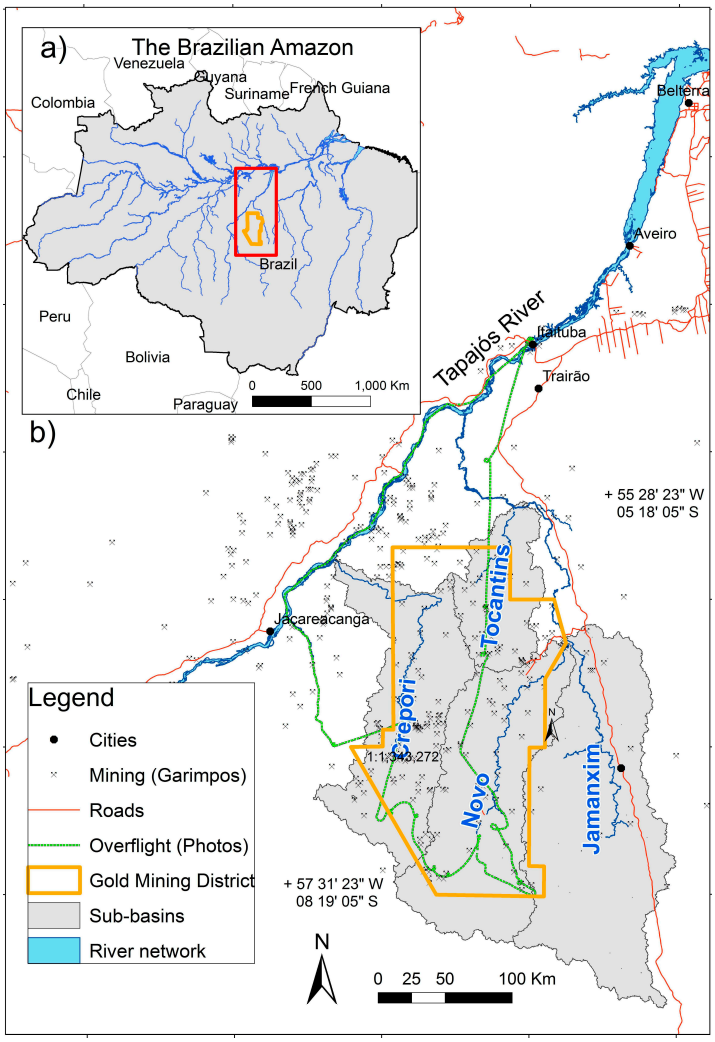

Figure 1. (**a**) Study area located in the Brazilian Amazon with indication of the Gold Mining District created in 1983 [6] by the Brazilian Federal Government. The four sub-basins of the Tapajós River Basin subject to this research are within: Jamanxim, Novo, Tocantins and Crepori sub-basins are depicted in (**b**), along with mining sites, roads, river network, and overflight path for aerial photos used in the land-cover validation process.

This region has been subject to high investments on agri-business and mining, resulting in several social conflicts for the access to natural resources and protected lands. Currently, more than

300 small-scale mines, with the participation of more than 50,000 miners, produce gold within three main sub-basins: the Novo, the Crepori, and the Tocantinzinho (abbreviated to Tocantins) [4,16]. For comparison purposes, another sub-basin (Jamanxim), characterized by low mining activity and high deforestation rates, was also included in the study area (Figure 1b).

3. Material and Methods

The methods used in this research involved six steps (Figure 2): (i) The building of the database including satellite images (1973–2012), aerial photos and auxiliary data (river network, soil type, etc.); (ii) Radiometric and atmospheric correction of satellite imagery having dark vegetation was used as a reference to create a normalized time-series for land use and water siltation detection; (iii) Mapping the gold mining area of the four sub-basins in 2012 based on the IRS/LISSIII images and validated with aerial photos; (iv) Classifying the historical Landsat images (2001, 1993, 1984 and 1973) and generating historical maps of mining area distribution using the 2012 map as a starting point; (v) Evaluating the influence of the historical mining area and sediment sources on satellite-derived historical water siltation (TSS, Total Suspended Solids concentration) from [16]; and (vi) Lastly, intersecting historical maps with the river network and soil type to assess possible sources of the sediment discharged into the rivers due to ASGM.

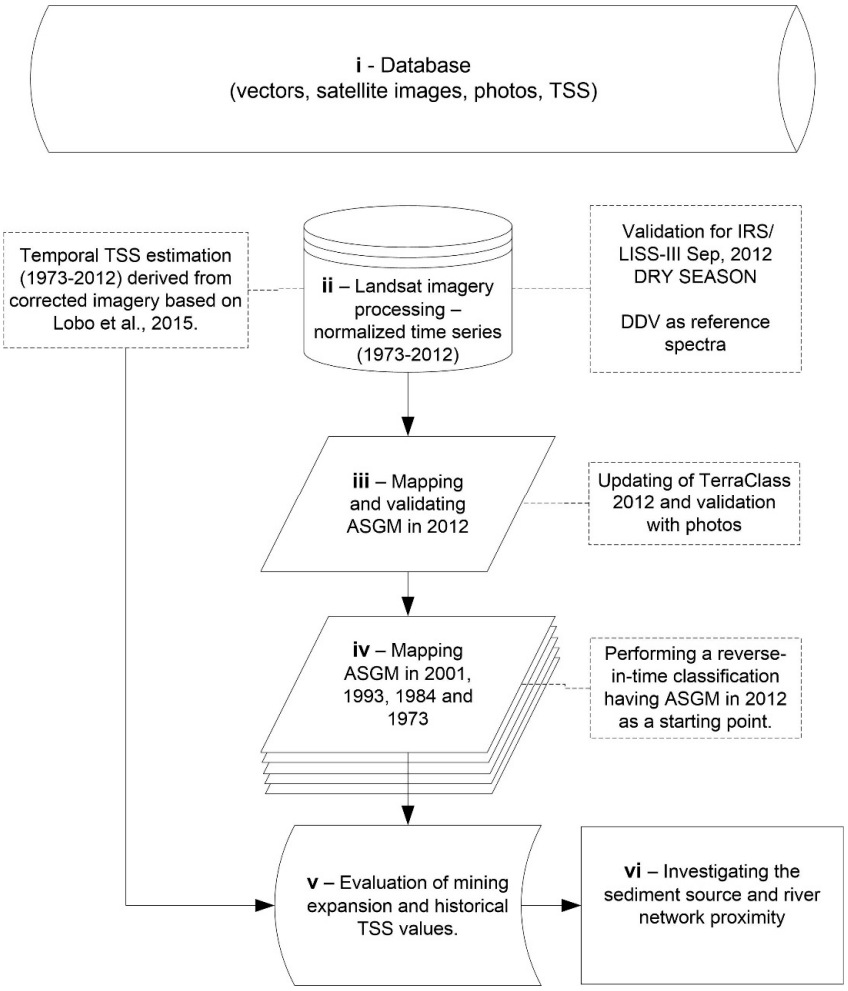

Figure 2. Flowchart of the methodology applied in this paper. (**i**) Database including satellite images, auxiliary vectors, photos and TSS from [12]; (**ii**) Landsat image processing to create a normalized time series from 1973 to 2012 from land use and water siltation extraction; (**iii**) Map ASGM in 2012 and validated with photos; (**iv**) Conducted a reverse in time classification of ASGM in 2001, 1993, 1984 and 1973; (**v**) Combined temporal analysis between TSS and ASGM expansion; (**vi**) Investigation of the sediment source resulted of ASGM activities.

3.1. Database

The database organized for this research includes (Table 1): satellite images from 1973 to 2012 for identification of mining areas; aerial photos taken to validate classification of ASGM in 2012; ancillary data such as roads, river network and mining sites to support ASGM identification; an official land-cover classification in the Brazilian Amazon provided by the TerraClass project; and historical TSS estimates for the main tributaries of Tapajós River from [12] (see Section 3.2).

Table 1. Description of the geographical database used including type of data, date of acquisition, general description, scale and source of data.

Type of Data	Date	Description	Scale/Resolution	Source
Satellite Images (5 tiles per date, raster files)	August 1973	Landsat 1 (MSS)	80 m	DGI/INPE [17]
	August 1984	Landsat 5 (TM)	30 m	
	September 1993	Landsat 5 (TM)	30 m	
	August 2001	Landsat 5 (TM)	30 m	
	September 2012	IRS/LISSIII	24 m	
Aerial photos	May 2012	Overflight performed in May 2012. Total of 40 photos and 70 mining polygons identified.		Shared by ICMBio
Ancillary data (vector files)	2013	River network	1:50,000	This study
	2010	Water Bodies	1:250,000	[18]
	2010	Roads	1:250,000	[18]
	2006	Soil	1:250,000	[19]
	2012	Mining sites and gold mining district	1:250,000	[20]
Land use classification (vector files)	2012	TerraClass Project classified land-cover use for the Brazilian Amazon.	1:50,000	Available at CRA/INPE [21]
Historical TSS concentration (raster files)	1973–2012	Estimation of TSS concentration for Tapajós River Basin retrieved from satellite images.	24–80 m	[12]

In order to have a land use classification for every decade since the 1970s using Landsat archive, five satellite image mosaics were constructed. The first set of images was acquired by the Landsat/MSS (Multispectral Scanner) in 1973. In the decades to follow, cloud-free images acquired by the Landsat/TM (Thematic Mapper) were available for the years 1984, 1993, and 2001. In 2012, a group of images acquired by the IRS/LISSIII (Indian Remote Sensing/Linear Imaging Self Scanning Sensor) was used as an alternative due to unavailability of Landsat images. The pixel size of utilized images ranged from 80 m (Landsat/MSS) to 24 m (IRS/LISSIII) (Table 1). For each mosaic, at least five tiles were downloaded from INPE/DGI and corrected for geographic, radiometric, atmospheric deviations and normalized according to methodology proposed by [19] (see Section 3.2).

An overflight performed in May 2012 by ICMBio agents (Brazilian National Agency of Protected Areas) involved collecting about 40 photographs for use in identification of mining activities within protected lands (see overflight path in Figure 1). These photos were shared with us (the authors), and a total of 70 polygons were used in this research to validate land-cover classification in 2012 based on IRS/LISSIII imagery. The visual identification of the polygons in the photos considered the spatial distortion caused by the oblique view of the camera used in comparison to the satellite images acquired with a perpendicular view (nadir).

To support ASGM and deforestation identification, several auxiliary data (vector files) were used such as roads, water bodies, gold mining district areas, mining sites and soil types. Except for the river network generated in this study based on SRTM images [22], all data derives from official national institutes in Brazil (Table 1).

As an attempt to classify and quantify the different land use in the whole Brazilian Amazon, the national government created the TerraClass project led by National Institute for Space Research

(INPE). The land use classification system follows the one recommended by FAO/UNESCO (Land Cover Classification System) and includes mining, pasture, agriculture areas, and secondary forest [23]. The classification is based on satellite imagery (usually Landsat archives) used for deforestation detection by PRODES program (Deforestation Monitoring Program in Brazil) and applies raster-based algorithms, such as Linear Spectral Mixing Models to map secondary forest [24], Normalized Difference Vegetation Index (NDVI) to map agriculture areas, and supervised classification Bhattacharya to map pasture areas. After mapping secondary forest, agriculture and pasture areas, the remaining deforested areas were classified into urban and mining regions based on visual interpretation of the satellite images used as background [21]. As the TerraClass classification is freely available at CRA/INPE [21] and represents one of the most important information sources for land use analysis in the Brazilian Amazon, it was used as a starting point to identify and quantify the mining and other land uses in 2012.

3.2. Imagery Time-Series for Monitoring Land Use and Water Quality Changes

To address the atmospheric correction and imagery normalization issues, the proposed method started with a set of images IRS/LISSIII acquired in September 2012, which were atmospherically corrected and validated based on in situ surface reflectance, ρ_{surf}, as described by [12]. The atmospheric correction was performed using a physical-based algorithm in FLAASH-ENVI [25] and considered ranges of water vapor values and aerosol optical thickness (AOT) from the closest AERONET (AErosol RObotic NETwork) station [26], near Belterra city (3°06′S, 55°03′W). After validation, the 2012 IRS/LISSIII images were used as reference for the inter-calibration of the historical Landsat images (MSS and TM). For Landsat-TM images acquired from 1984 to 2001, the atmospheric correction was performed with water vapor and aerosol optical thickness (AOT), optimized to match the DDV (Dense Dark Vegetation) spectra of those from previously corrected IRS/LISSIII.

Following the atmospheric correction of the imagery database, the DDV spectra from the historical images were extracted and compared with the reference images (IRS/LISSIII). The historical images in which $\rho_{surf(red)}$ did not fall within an acceptable range (up to 50% difference at red band, which corresponds to a difference of up to 1.5% in $\rho_{surf(red)}$) and were subjected to another iteration of atmospheric correction by optimizing the water vapor and visibility parameters (Figure 3a). The acceptable difference in threshold was defined for the red band since the red band of all the sensors used in this analysis present similar ranges (center at ~650 nm). Furthermore, the same image data set was processed for the water siltation analysis and the red band presented the highest correlation to increasing TSS [12].

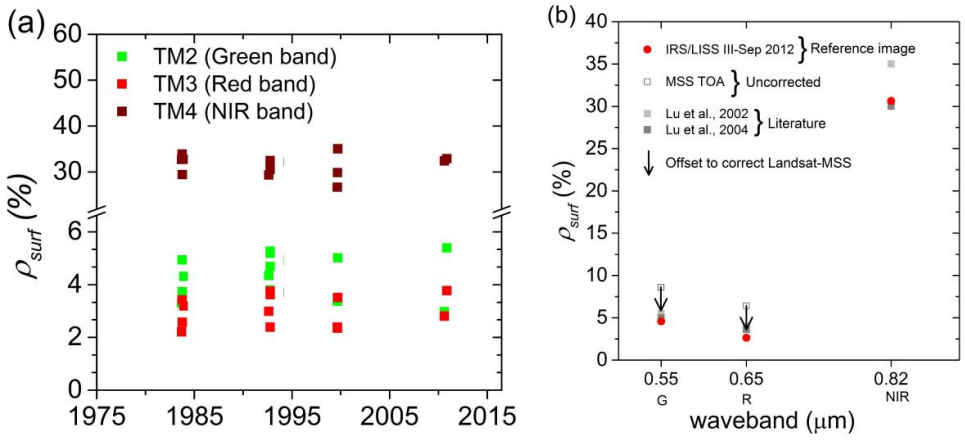

Figure 3. (**a**) DDV (Dark Dense Vegetation) spectra for dry seasons (August–October) extracted from historical Landsat-5 TM images having IRS/LISSIII spectra shown in (**b**) as reference; (**b**) DDV extracted from dry season (IRS/LISSIII) used as reference for optimizing atmospheric parameters on Landsat historical data. Examples of uncorrected Landsat 1-MSS (ρ_{TOA}), and dense forest from the Brazilian Amazon found in literature using Landsat TM data [27,28] are also shown. Adapted from [12].

Landsat 1-MSS specifications were not available for the physical method employed in the atmospheric correction of the other images. As such, the Landsat 1-MSS images (1973) image sets were radiometrically corrected to reflectance at the Top-of-Atmosphere (TOA), ρ_{TOA}. The atmospheric effects were corrected by applying offsets only at the green and red bands (Figure 3b), since the MSS infra-red waveband (750 nm) is not comparable to those from Landsat-TM and IRS/LISSIII centered at 820 nm. Once all the images were corrected and inter-calibrated, the analysis of land use (Sections 3.2 and 3.3) and water siltation (Section 3.2) temporal detection was performed.

Historical Total Suspended Solids (TSS) Estimated from Normalized Imagery Time-Series.

The historical variation of TSS along the Tapajós River and main tributaries were extracted from [12] for the same period used in this paper (1973–2012), after an extensive sampling of water bodies impacted and non-impacted by gold mining tailings.

The relationship between TSS and satellite data (surface reflectance at red band, $\rho_{surf(red)}$) was established after two field campaigns performed in April 2011 (high water level) and September 2012 (low water level) in the Tapajós River and main tributaries for TSS and surface reflectance measurements. Two sets of satellite images were acquired and calibrated during the field campaigns, using the in situ data (water surface reflectance at red band) as ground truth. As TSS increases, the $\rho_{surf(red)}$ increases according to the power function depicted in the Figure 4.

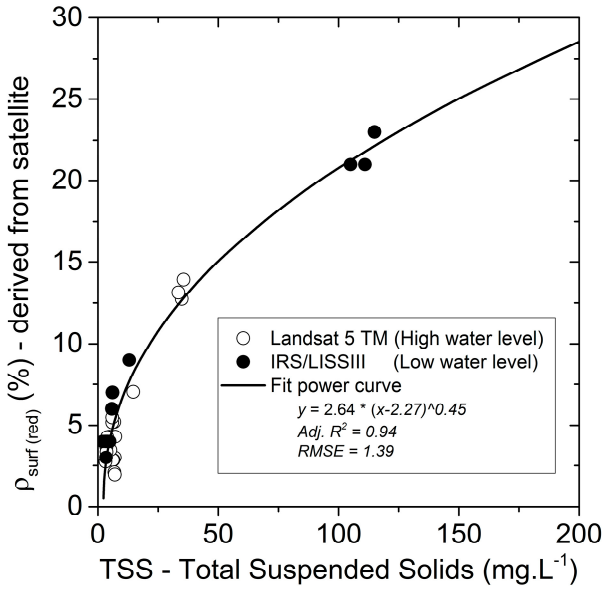

Figure 4. Non-linear fit between TSS (n = 39, Adj. R^2 = 0.94, RMSE = 1.39) and reflectance (red band) derived from satellite sensors (Landsat TM data for high water level, April 2011; and IRS/LISSIII data for low water level season, September 2012). Adapted from [12].

The historical water siltation estimation corresponds to the low water level period, as that is the time of year when mining activities are most intense [12]. The Landsat MSS (1973), TM (1984–2001) and IRS/LISSIII (2012) images were corrected for atmospheric and sun-glint effects, and $\rho_{surf(red)}$ at red band was used to retrieve TSS concentrations (mg$\cdot$ L^{-1}) based on this empirical equation [12].

3.3. Mapping Mining Areas in 2012

Prior to having the 'ground truth' information for validation purpose of mining areas in 2012, we first analyzed the aerial photos to identify the polygons of ASGM and other land uses. A total of 70 polygons were identified in the photos, varying in size and shapes, and were used for validation of ASGM and other uses in 2012 (Figure 5). The scheme of land-cover classification used throughout this paper was defined as: (1) ASGM, which includes all land use related to active or inactive mining

operations, such as mining areas themselves, airstrips, degraded areas, mining-related ponds, mining settlements; and (2) deforested areas that are not associated with mining, which includes pasture and other agriculture-related areas. Along with users' expertise in visual identification of mining areas in the IRS/LISSIII image (2012), the mapping process used auxiliary information such as *garimpos* distribution, roads, and other secondary information for a more accurate identification. All the visual interpretations of land use between ASGM and others were based on RBG composition (R/G/B: Red/NIR/Green bands) where ASGM followed an irregular pattern, bright signal (white), and mostly along the drainage network (Figure 5bi). On the other hand, other uses such as pastures present a regular shape; usually, between the drainage network, and not as bright as ASGM areas because of the presence of grass and other vegetation (Figure 5bii).

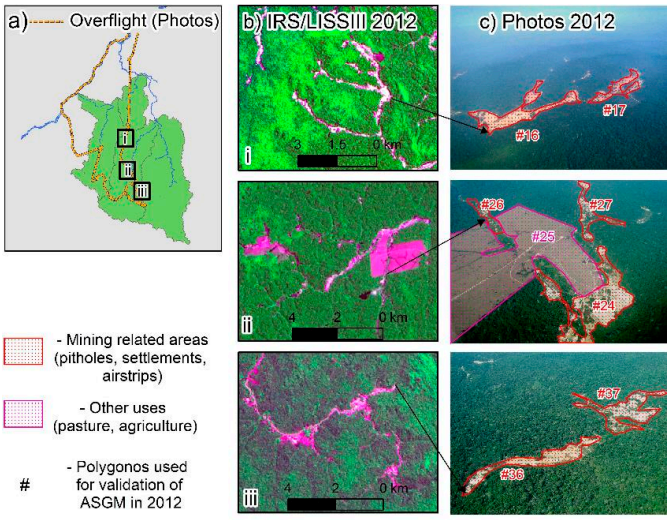

Figure 5. (**a**) An overflight was taken in the study area to identify ASGM and validate classification of land use based on IRS/LISSIII images (R/G/B: Red/NIR/Green bands) (**b**). Examples of eight polygons extracted from three different areas (**i**–**iii**) includes mining-related areas (**in red**) and other land uses that are not associated with mining (**in purple**). The visual identification of the polygons in the photos taken in 2012; (**c**) considered the spatial distortion caused by the oblique view of the camera used.

To identify the small-scale gold mining in the whole study area in 2012 using satellite images, the initial step that was considered was the usage of the TerraClass maps (named as *TerraClass-2012*), which provides land use classification for the Brazilian Amazon in 2012 (Table 1). We considered the use of *TerraClass-2012* as a starting point in identifying and mapping ASGM distribution in 2012 as it is an official classification that is freely available, and provides land use validated with field works. As the TerraClass project covers the whole Brazilian Amazon on a large scale, it lacks in detecting very small mining areas. To overcome that and provide an up-to-date identification of ASGM in 2012 (named as *MapASGM-2012*), *TerraClass-2012* was set as a base classification to guide the manual vector editing having the satellite image IRS/LISSIII acquired in 2012 as background. Then, validation of both *MapASGM-2012* and the *TerraClass-2012* maps took place with the 70 polygons of different sizes corresponding to mining and deforested areas identified in the aerial photos.

3.4. Mapping Mining Areas in 2001, 1993, 1984, and 1973

The procedure to generate the time series of mining area expansion followed a 'reverse-in-time' approach, having started with the use of the validated *MapASGM-2012* as a reference for the identification of the mining areas in the 2001 Landsat images. Repetition of the same procedure occurred for the other dates: 1993, 1984 and 1973. This procedure relies on the assumption that ASGM changes in the land cover are severe and remain detectable from satellite sensors for decades (Figure 6).

In most cases, once there was an ASGM mining site in the past, it is likely to have remained a mining site to the present day.

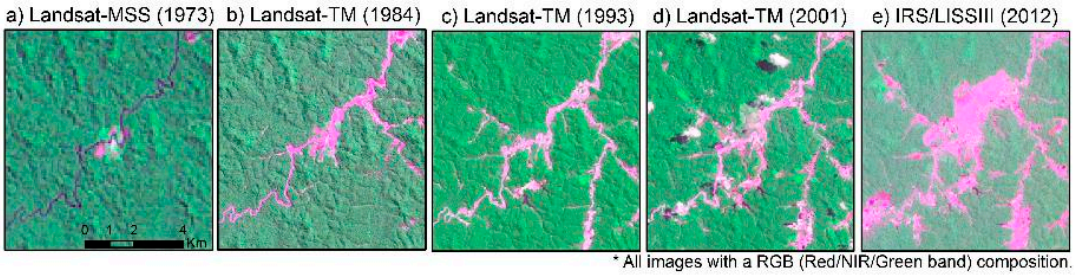

Figure 6. Example of how severe ASGM land changes remains detectable by satellite images. It also illustrates ASGM expansion over the decades from 1973 (**a**); 1984 (**b**); 1993 (**c**); 2001 (**d**); to 2012 (**e**). RGB composition of Landsat and IRS/LISSIII images.

The up-to-date validated *MapASGM-2012* can be used as a guide for mapping ASGM in the previous decades when no information for validation purposes is available. For example, to distinguish ASGM and deforested areas in 2001 (Figure 7a), an unsupervised classification (IsoData) using red and near-infrared bands was conducted to detect all land-cover use that is not forest into one class (named as *land use mask 2001*) (Figure 7b). In order to distinguish mining and deforested areas properly, this *land use mask 2001* was intersected with the *MapASGM-2012* (Figure 7c) followed by a precise manual vector editing at 1:25,000 scale to incorporate land use areas that were not included in the intersection with 2012, such as the case of regrown secondary forest, resulting in the *MapASGM-2001* (Figure 7d). The manual vector editing, based on visual interpretation and ancillary data, is also essential in assigning the correct classification in the case of the areas, which had been converted, to other land uses. Once the *MapASGM-2001* is completed, the same process (steps Figure 7a–d) was repeated for the remaining years (1993, 1984, and 1973) for the sub-basins of study: Crepori, Novo, Tocantins, and Jamanxim (Figure 1).

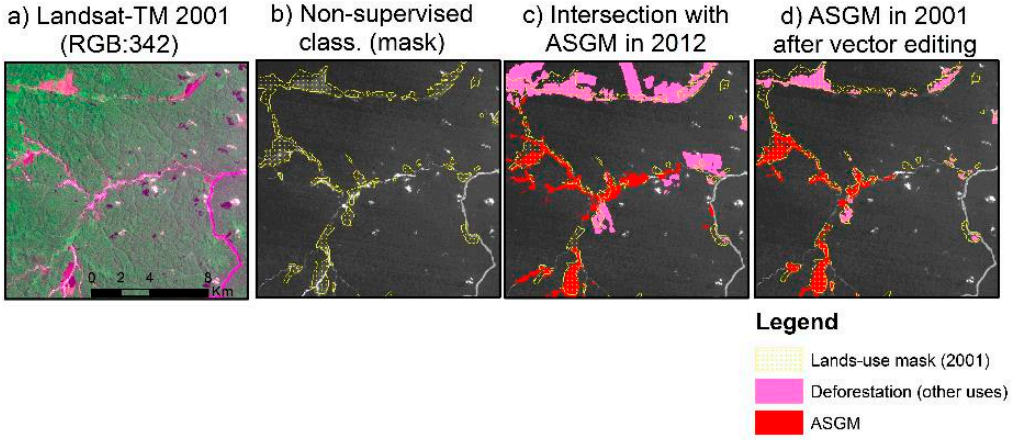

Figure 7. Mapping mining areas (and deforested areas that are not mining) using Landsat historical images (2001, 1993, 1984, and 1973). Satellite image database in 2001 (R/G/B: Red/NIR/Green band) (**a**) was submitted to an unsupervised classification where all land use classes, except forest, are included into one class, creating a *land use mask 2001* (in **yellow**) (**b**). This mask was then intersected with the *MapASGM-2012* (**c**) followed by a vector editing in order to include all mining (**red** polygons) and deforested areas (**pink** polygons) in 2001 resulting in the *MapASGM-2001* (**d**). The same procedure was applied to the imagery Landsat-TM database in 1993, 1984, and Landsat-MSS data in 1973.

3.5. Relationship between Historical Mining Areas and Water Siltation

Since neither historical nor present data on sediment transport of mining tailings into the river network is available, the historical mapped mining areas were spatially associated with corresponding satellite-based water siltation (total suspended solids-TSS) from [12] for the tributaries, Jamanxim, Crepori, Novo, and the Tocantins. Further investigation of spatial and temporal effects of ASGM on water siltation were conducted based on the land use dynamic (generated in this paper), mining techniques [29], gold production [6], and socio-economic framework [30,31] throughout the decades.

3.6. Investigating the Source of the Sediment Derived from ASGM

To assess the source of the sediment carried from mining areas to the drainage, the temporal gold mining areas were overlayed with thematic maps such as soil type and connectivity with the river network. The map relating to soil type, from the Brazilian national classification [24] in a 1:250,000 scale, was clustered according to the international classification [32] in order to be comparable to other research around the world. Buffering-zones (100, 250, 500 and 1000 m) along the river network (generated in this study, scale 1:50,000) were created to define proximity of mining area to the river network. According to the recent New Forest Code (National Law n°12.651/2012), a buffer distance of at least 100 m from rivers with a width between 50 and 200 m is permanently protected by law and no kind of land use is allowed because it directly affects water quality. Similarly, buffering-zones were created along roads [18] in order to investigate their relevance to water siltation.

4. Results

4.1. Validating Gold Mining Area in 2012

The polygons identified in the photos were used to validate the land use cover classification in 2012. According to the validation matrix (Table 2), the *TerraClass-2012* underestimated the mining area. *TerraClass-2012* failed to classify mining in 21 out of 53 polygons that are identified as ASGM in the photos, with an overall accuracy of 64% (Table 2). The validation of the *MapAGSM-2012* classification showed that the overall accuracy increased to 93%, since manual editing included mining areas of different sizes from very small (5 ha) to exceedingly large (1000 ha), and updated mining areas in 2012. Omission errors total 6% (3/53), whereas commission errors are less than 4% (Table 2).

Table 2. Matrix of validation of *TerraClass-2012* and *MapASGM-2012* land use classification having aerial photos as ground-truth. Overall accuracy is 64% for *TerraClass-2012* and 93% for *MapASGM-2012*.

Classification of *TerraClass-2012*					
		Mining	**Others Uses**	**Not Classified**	**Total**
photos	Mining	32	13	8	53
	Others uses	3	14	0	17
	Total	35	27	8	70
Classification of *MapASGM-2012*					
		Mining	**Other Uses**	**Not Classified**	**Total**
photos	Mining	50	3	0	53
	Other uses	2	15	0	17
	Total	52	18	0	70

Figure 8 depicts one example of omission error and another example of misclassification of the *TerraClass-2012* in comparison to the updated *MapASGM-2012*.

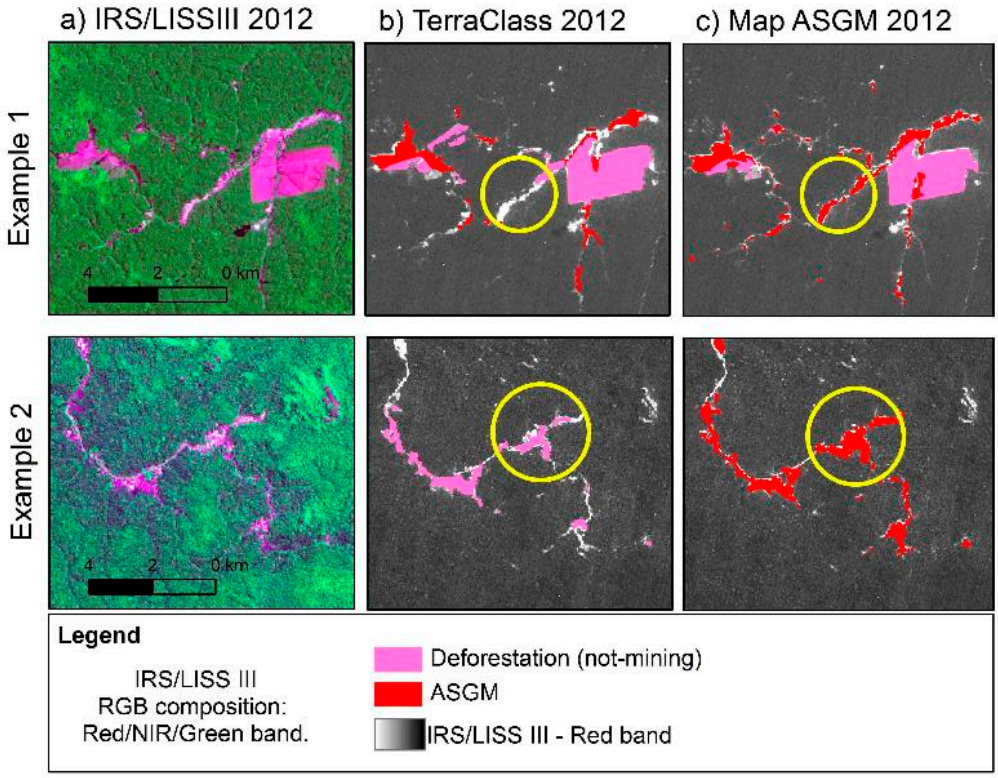

Figure 8. (**a**) The IRS/LISSIII was used as a background image to support ASGM identification in 2012. Examples of performance of *TerraClass-2012* (**b**) and updated *MapASGM-2012* (**c**), are given in two image subsets to illustrate the omission (Example 1) and misclassification errors (Example 2) observed for *TerraClass-2012* in comparison to updated *MapASGM-2012* (yellow circles).

4.2. Gold Mining Area from 1973 to 2012

The satellite-derived mining area in the four sub-basins of study during the past 40 years—1973, 1984, 1993, 2001, and 2012—are presented in Figure 9 and Table 3. In 1973, dominant forested conditions were observed with a mining area of 15.4 km^2 (0.03% of the total area of study), mainly limited to the Crepori (6.3 km^2) and Novo (7.0 km^2) sub-basins. Eleven years later, the mining area increased to 47.5 km^2 (0.09% of the total area), and again the Crepori and the Novo sub-basins showed the largest mining areas with 22.8 and 16.1 km^2, respectively. In 1993, the mining area tripled to 166.3 km^2 (0.30% of the total area), with the Crepori sub-basin alone showing ASGM up to 77.0 km^2, followed by the Novo (69.2 km^2), the Tocantins (11.9 km^2), and the Jamanxim (8.2 km^2). Contrary to the trend in previous decades, the next decade (to 2001) saw the total mining area increase only slightly, to 171.7 km^2 (0.31% of the total area). The stagnation period during the late 1990s and early 2000s rapidly changed within the following decade, resulting in an increase in the mining area to 261.7 km^2 (0.48% of the total area) in 2012. It is interesting to point out that the Jamanxim sub-basin, while presenting the lowest mining area, had the greatest deforestation rates throughout the five-decade period (20% of the total area in 2012), mostly along the BR-163 (South-North) highway.

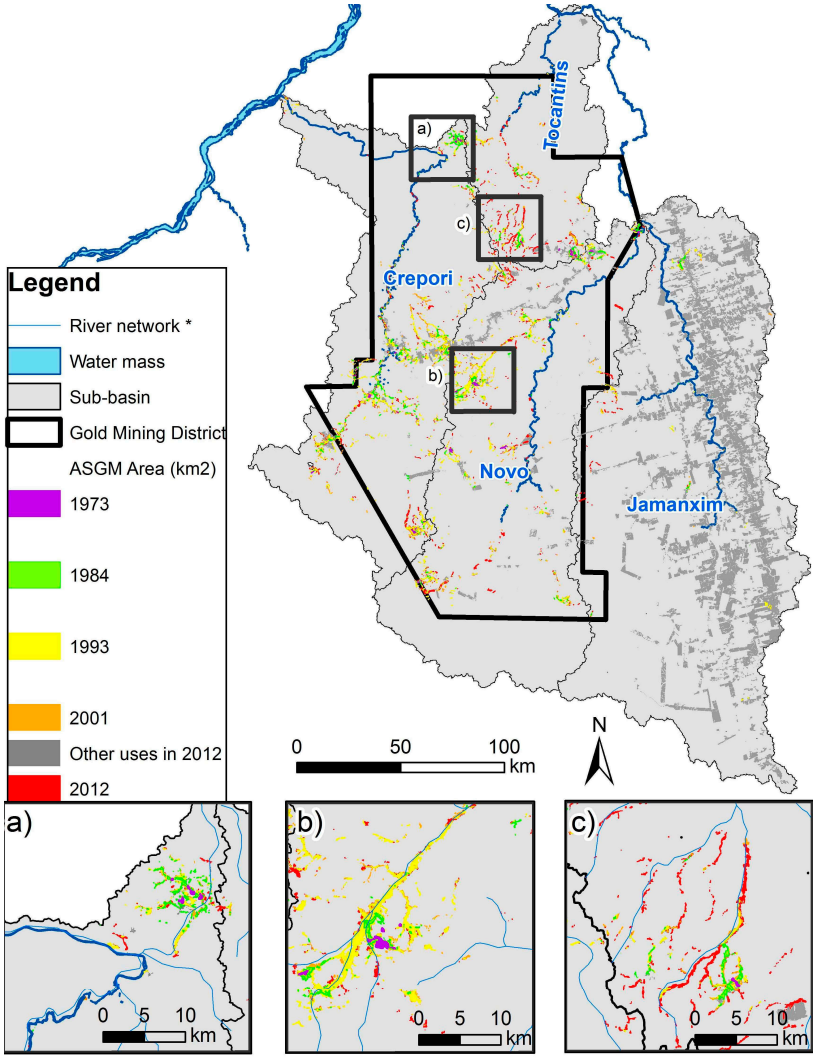

Figure 9. Map of the ASGM expansion (1973, 1984, 1993, 2001, and 2012) in the area of study. Note that the expansion occured during different periods at different regions: for Cuiú-cuiú area (**a**) encountered the highest expansion occured until 1984; for the Surubim area (**b**), most of the expansion happened between 1984 and 1993; and for the Tocantinzinho area (**c**) the expansion is more prominent between 1993 and 2012. Other land uses in 2012 are also plotted in dark gray. * River network only displayed on (**a**–**c**).

Table 3. Tabulation of historical ASGM and other uses not including mining for the four sub-basins of study: Crepori, Novo, Tocantins and Jamanxim.

Mining Area (km^2)					
	Jamanxim	**Crepori**	**Novo**	**Tocantins**	**Total**
1973	0.1	6.3	7.0	2.0	15.4
1984	2.2	22.8	16.1	6.3	47.5
1993	8.2	77.0	69.2	11.9	166.3
2001	7.3	77.9	63.1	23.3	171.7
2012	10.9	115.5	96.2	39.1	261.7
Other uses (km^2)					
	Jamanxim	**Crepori**	**Novo**	**Tocantins**	**Total**
1973	3.8	0.5	0.5	0.0	4.8
1984	185.1	11.7	10.2	2.9	209.9
1993	579.2	52.5	62.8	14.6	709.1
2001	1338.2	69.2	107.3	38.8	1553.5
2012	4212.0	192.2	365.7	54.9	4824.8

4.3. Historical Gold Mining Area and Water Siltation

The historical gold mining area maps, along with historical TSS concentration from [12] were combined in order to investigate the temporal relationship between mining area expansion and water siltation in the four tributaries: Jamanxim, Crepori, Novo, and the Tocantins sub-basins. Figure 10 shows the percentage of ASGM increase between 1973 and 2012 calculated as $(A_1 - A_0)/A_0$, where A_0 is the ASGM area at the initial date and A_1 is the ASGM area in the following decade, plotted along with historical TSS concentration.

Although other uses prevail and mining activity does occur in very small areas in the Jamanxim River sub-basin, the impact on water siltation is relatively minor compared to the other basins and TSS remains under 5 mg· L^{-1} throughout the period studied (Figure 10d).

In Crepori and Novo rivers, the ASGM started with a few mining locations in 1973, with no resultant perceived impact on water turbidity; TSS concentrations were <5.0 mg· L^{-1}, similar to upstream Jamanxim which can be considered relatively pristine in regards to ASGM. However, in 1984, mining areas increased by about two to three times for the Novo and Crepori rivers, respectively, and within that period, high TSS concentrations were observed corresponding to >50 mg· L^{-1} for Crepori, and >15 mg· L^{-1} for Novo (Figure 10a,b).

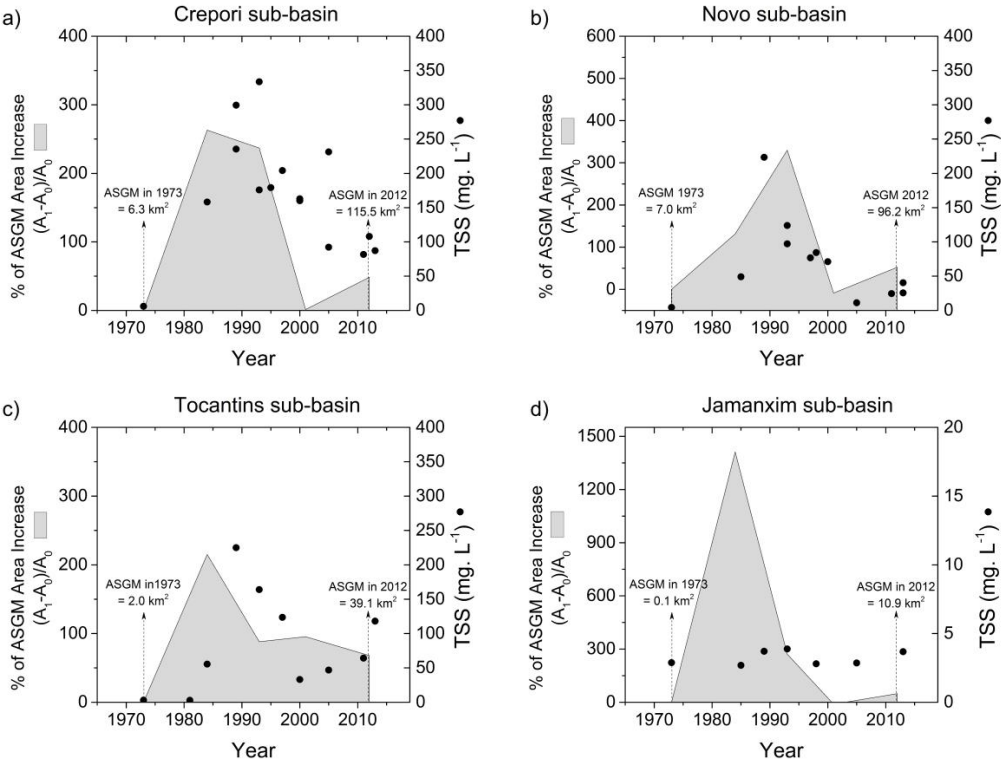

Figure 10. Percentage of ASGM area increase from 1973 to 2012 plotted along with historical TSS derived from [12] for the four sub-basins studied (**a**–**d**). Note different TSS scale for the Jamanxim River Basin.

In the early 1990s, the Crepori and the Novo rivers exhibited a similar trend; TSS concentration was above 100 mg· L^{-1}, while mining areas increased from around 20.0 km^2 to 75.0 km^2 in both sub-basins. In the Tocantins sub-basin, the increase in mining area was less abrupt than in the Crepori and Novo sub-basins until the late 1980s. However, in 1989 the TSS concentration increased to concentrations as high as 220.0 mg· L^{-1}, indicating a significant increase in mining activities in the Tocantins sub-basin during this period (see Figure 11 for TSS maps).

The period between 1993 and 2001 shows scant expansion of the mining area in the sub-basins as seen in Figure 10. For all impacted sub-basins, a tendency of TSS reduction was observed during this period of ASGM recession. Even with reduction of mining expansion, the TSS values do not

return to initial values in 1973 (TSS < 10 mg· L^{-1}) indicating that gold mining kept active, or even that inactive degraded areas (mining tailings) could still contribute to the high TSS values observed.

However, the recent gold rush, occurring over the past 10 years (represented by the percentage of gold mining area increase from 2001 to 2012), has influenced TSS concentrations. The Novo and the Tocantins rivers showed increasing TSS concentrations (mg· L^{-1}) in this period. This tendency was not observed for the Crepori, but this tributary still presented high TSS concentrations (around 100 mg· L^{-1}) throughout the past decade (Figures 10 and 11).

Figure 11 shows the spatial and temporal distribution of TSS along the Tapajós River (Figure 11a) and the Jamanxim River (Figure 11b) with indication of its main tributaries, and illustrates the TSS variation observed in Figure 10.

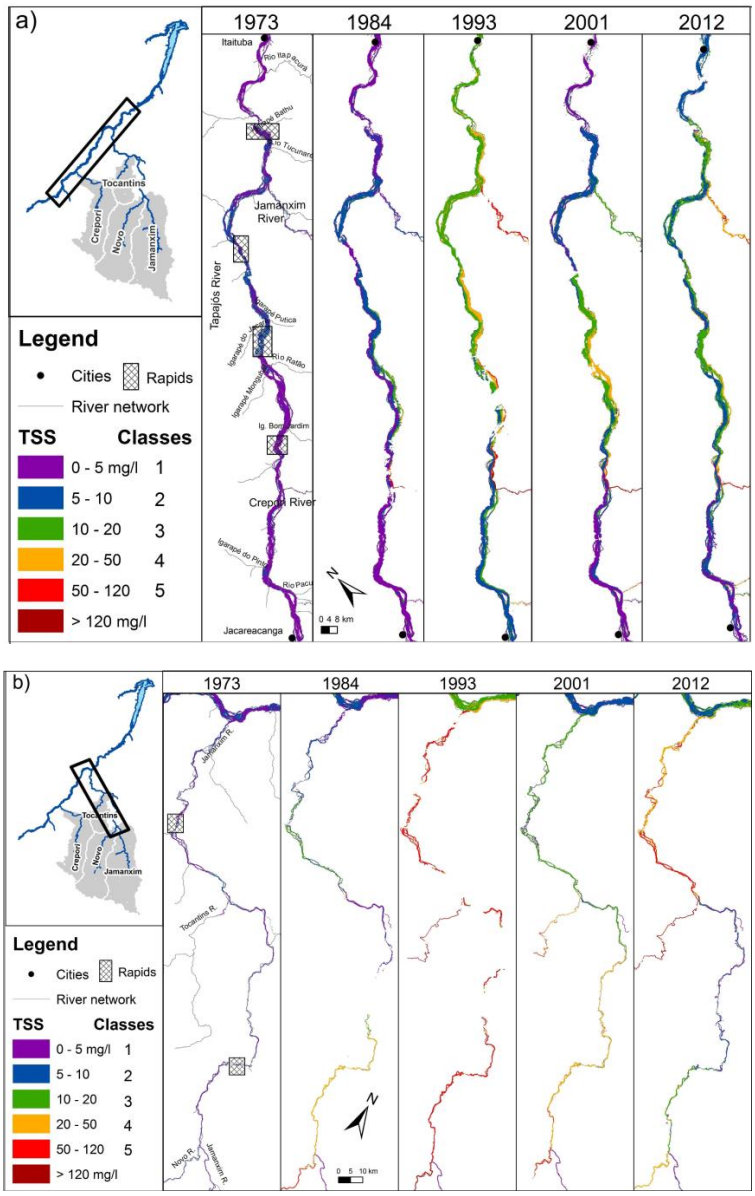

Figure 11. Spatio-temporal distribution of TSS along the Tapajós (**a**) and Jamanxim rivers (**b**). Sections of the river with rapids that often cause water mixing are also indicated. TSS maps based on five mosaics of satellite images: 1973 (Landsat-MSS), 1984, 1993, 2001 (Landsat-TM), and 2012 (IRS/LISSIII). All images are from the dry season (August to October); see [12] for more information.

4.4. Characterization and Distribution of Gold Mining Area: Proximity to Roads and Drainage Network, and Soil Types

The quantification of the mining area along the river network buffer zones showed that, in 2012, 40% of total mining areas were within a 500 m distance from the river network (Figure 12). Moreover, within the first 100 m, ~9% of the total mining area was mapped in 2012. Together with the increment of the total mining area over the years, the percentage along the river network also increased from 1973 to 2012. As an example, within the first 500 m from the river network, we found 12% of ASGM in 1973, and 31% in 1984. In the years 1993 and 2001, the percentage was similar to that of 2012 (40%), which indicates that the mining area increment in 2012 followed a pattern of gold exploitation similar to that of the previous two decades. Mapped mining areas are not predominantly located along the road network. For instance, approximately 5% of the total mining area in 2012 was mapped within a buffer of 1000 m along the roads, mostly along the 'Trans-Garimpeira' road (East-West). On the other hand, the distribution of other land uses are highly associated with the road distribution as evident in the Jamanxim basin with deforestation areas along the BR-163 (North-South) [31].

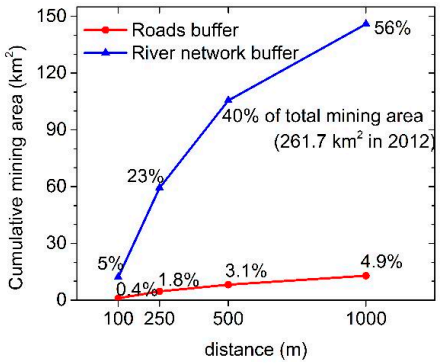

Figure 12. Cumulative mining and deforestation areas for 2012 along river and road buffer zones for 100, 250, 500, and 1000 m.

The intersection of the most recent gold mining map over the soil type map [32] indicates that mining predominantly occurs in ferrasol soils (Table 4). Overall, ferrasols are characterized with high clay content (up to 70% of total weight) and covers more than 90% of the study area. Another heavily mined area occurs in gleysol soils related to alluvial systems. Gleysols are generally also clay-rich, but with higher water content as they are subject to flooding several months a year.

Table 4. Tabulated mining area in 2012 over different soil types according the international classification [32].

Soil Type (World Reference Base, 1998)	Mining Area in 2012 (km^2)
Acrisol	1.2
Arenosol	2.6
Gleysol	53.7
Ferrasol	180.5

5. Discussion

5.1. Satellite Imagery Time-Series for Estimation of Land Use and Water Siltation Change

The proposed inter-calibration of historical imagery, using DDV as a reference target, demonstrated that forest spectra from historical Landsat-5 TM (1984–2011), behaved as an invariant spectral feature over decades (Figure 3). Consequently, the $\rho_{surf}(\lambda)$ variation observed for mining areas and water bodies were attributed not to environmental conditions but only to the land use change

and to variation in optical constituents in the water, respectively [12]. These procedures provided the necessary normalized database for a complete investigation on the impacts of ASGM expansion on the water siltation extracted from the same imagery database in the Tapajós River Basin.

The ASGM area distribution in 2012 was identified and quantified based on IRS/LISSIII images. We demonstrated that the TerraClass classification failed to classify small mining areas, and misclassified other polygons to other uses when validated with photos. To address this issue, a complete update of the *Terraclass-2012* occurred based on the brightness (spectra), shape, and location criteria for identification of ASGM (Figure 5) in comparison to other uses, such as pasture, resulting in the *MapASGM-2012*. Based on the fact that ASGM remains detectable for several decades by satellite images (Figure 6), the proposed methodology provided reliable classification to perform reverse-in-time identification and quantification of ASGM (2001, 1993, 1984, and 1973) imagery dataset having the MapASGM-2012 as a starting point (Figure 7). Although this method requires user training for proper identification of ASGM, it can be conducted with only a few steps and provides a reliable quantification and distribution of ASGM in the Amazon.

The imagery-derived TSS from the Tapajós River Basin [12] suggests that its variability is mainly affected by the concentration of inorganic suspended solids and is also increased due to mining activities. We observed that the possible increase in TSS caused by deforestation is not at the same magnitude as the increase in TSS caused by mining activity. For example, the Jamanxim River, which is characterized by highly deforested areas but with low mining activity, presented low TSS values. Generally, the natural clear water condition of the Tapajós River Basin [33] facilitates the detection of sediment plume caused by gold mining as opposed to naturally white water rivers which also receives mining tailing, such as the Madre de Dios River in Peru.

The whole methodological approach of creating a normalized (inter-calibrated) time series, followed by a simultaneously extraction of land use and water siltation change, provided very satisfactory information for a further discussion on the ASGM impacts on the water quality changes over the decades.

5.2. Spatio-Temporal Analysiof ASGM and Water Siltation (1973–2012)

The spatio-temporal extent of ASGM and its relationship with river water siltation is discussed in a chronological order considering the history of gold exploitation and the physical processes of sediment transportation (mining methods, and soil type) that affect water siltation of the Tapajós River system. Combining the historical context of mining activities from [5,8] and data from this research, four main periods of ASGM in this region were identified (Figure 13):

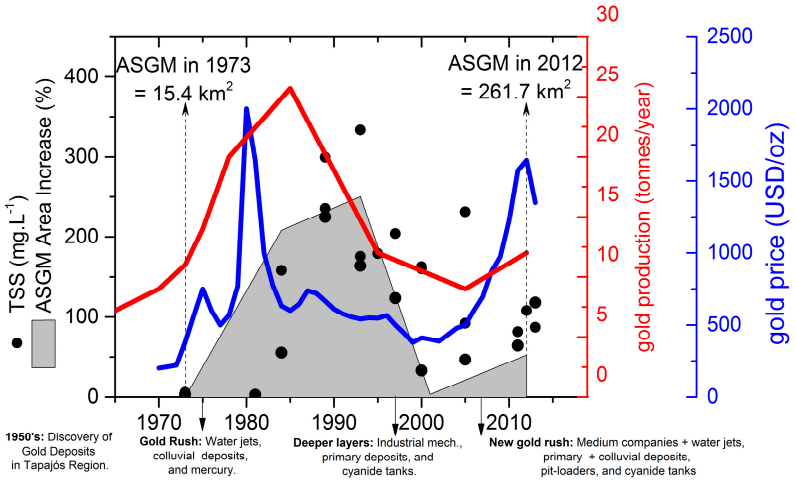

Figure 13. Plot of the percentage ASGM for the whole study area, along with the TSS concentration at the Crepori and Tocantins rivers, gold production in tonnes/year [4] in the Tapajós Area, and gold price (USD/oz) adjusted for inflation from 1970 to 2013 [34]. Chronological events of mining techniques, type of gold deposits exploited and type of miners are indicated by the arrows. Adapted from [12].

Period from the 50s to mid-70s—As an alternative to the decline of latex production, the first ASGMs were established around 1958 along the Tropas and the Crepori rivers [29]. Following the National Integration Program [35,36], the next decade experienced the construction of several highways crossing the Brazilian Amazon, such as the Cuiabá-Santarém Highway (BR-163) [31]. These investments encouraged a significant migration from the northeast region of Brazil to the Tapajós River basin to start new mining pits. As a result, in the early 1970s the estimated area of ASGM was approximately 15.4 km^2 (Table 3), with a gold production of 5 tonnes/year, approximately [5,7,8].

Until 1977, ASGM exploited mostly the alluvial deposits of secondary gold ore by manual and rudimentary methods, such as those involving the use of pans and picks [29]. The low capacity of ore processing during this period explains the observed low water siltation impact observed. TSS concentrations lower than 5.0 mg$\cdot$L^{-1} were estimated for the Crepori River (Figure 10a), similar to the expected concentrations for 'clear water' according to the Amazonian water classification scheme [37].

Satellite-based estimated TSS concentrations in 1973 data for the remaining tributaries were contaminated by radiance adjacency effect [12] due to MSS image pixel size (80 m). Despite potential uncertainty of the 1973 satellite-based estimates for narrow rivers, the estimated TSS concentrations were similar to those of Crepori and upstream Tapajós River, thus corroborating that the establishment of ASGM (15.4 km^2) and employed techniques from 1958 to 1973 resulted in low water siltation impact.

Period from late 70s to early 90s—As a result of the introduction of a new low-budget technology based on the use of water-jets and rafts, and the concurrence of factors such as high gold prices and government support [4,5], the following decade had considerable spatial expansion of all mining locations. Our data shows that in 1984, ASGM area corresponded to 47.5 km^2 and in 1993 (166.3 km^2) maps showed a spatial expansion of all mining locations compared with the 1973 map (15.4 km^2) (Figure 9 and Table 3). This period corresponds to the peak of gold mining production (on average, 20 tonnes a year), when approximately 100,000 *garimpeiros* were reported in the studied region [4,5]. It is important to note that most of this ASGM expansion occurred along the river network. In 1993, for example, 55% of the mining areas were located within 1000 m of the river network (Figure 12) and it is worth noting that the soil type in the alluvial is mostly gleysol (Table 4), with high amounts of clay (>70%) and inorganic fine particles that remain suspended in the water for many kilometers [38]. Other studies mapping ASGM in the Amazon also indicate that most of the mining areas are distributed along the river network with high potential for direct impact on the aquatic system [38–40].

In the sub-basins where the ASGM area increased, the TSS increased more than one order of magnitude. For example, in the Crepori River, TSS increased from 6.5 mg$\cdot$L^{-1} in 1973 to over 200.0 mg$\cdot$L^{-1} between 1989 and 1993 (Figure 10). The effects of ASGM were also observed for the Novo and the Tocantins rivers, where TSS increased to levels above 100 mg$\cdot$L^{-1} during the same period (Figures 10 and 11).

The impacts of increased water siltation on these aquatic environments are numerous. Increased water siltation has a strong impact and direct consequences for how light is attenuated in the water and consequently the depth of the euphotic zone. For instance, Lobo et al. [41] have defined that in the Tapajós River basin, the euphotic zone can decrease from 6.0 m to 1.0 m in non-impacted and ASGM impacted rivers, respectively. These changes can potentially change the phytoplankton community [41], and primary production [42].

It is worth noting that, in the Jamanxin sub-basin, high rates of deforestation rates were observed, increasing from 3.8 km^2 in 1973 to 579.2 km^2 in 1993, but impact on the TSS was not identified, since concentrations were lower than 5.0 mg$\cdot$L^{-1} for all years (Figure 10). Although a few studies show that other uses such as pasture and agriculture fields can have an impact on the water quality [43–45], considering the dataset of the case of Tapajós River Basin, water siltation caused by other uses can be assumed to be negligible when compared to water siltation caused by ASGM.

Period from mid-90s to mid-2000s—the high spatial extension of ASGM areas and associated increase in TSS concentrations in the rivers observed in the previous period changed to a more

stagnant condition in the following decade (Figure 10). From 1990 to 2000, gold production in this region decreased gradually from approximately 20 to 8 tonnes per year due to a reduction in the international gold price in the principal stock markets around the world [8]. In addition, the exhaustion of easy-access alluvial and colluvial gold deposits forced the miners to start exploiting primary deposits of gold, which require high mechanization levels and an increase in the costs of production [8]. These factors contributed to the observed minimal change in ASGM area and the decrease in suspended sediment in the riverine waters. Consequently, TSS was reduced by half or more in comparison with the previous decade in all impacted rivers (Figures 10 and 11). Estimated TSS concentrations were still much higher than the initial period. This is likely a result of (although reduced) still active ASGM [46], as well as a result of mining tailings derived from abandoned mining areas (degraded areas). For the Jamanxim River, neither the sparse ASGM nor the very high deforestation rate from 1993 to 2001 showed any significant effects on TSS concentrations.

Period from mid-2000s to present—A new gold mining rush characterizes this period, when an increase of 50% in ASGM was observed from 2001 (171.7 km^2) to 2012 (261.7 km^2). Encouraged by the new rise in the price of gold, the Tapajós region has attracted significant investments by medium/large national and foreign companies to extract primary gold in rock deposits with the use of pit-loaders, heavy mills and trucks, characterizing a new period of 'industrial' mining [29]. Presently, about 35 negotiations have been conducted (joint ventures) involving 19 mining companies [4]. This type of mining operation requires higher mechanization levels with the use of several load pitchers (approximately 50, according to the local environment protection agency, ICMBio) and cyanide tanks.

Within this period, the economic scenario has been very favorable, not only for companies exploiting primary deposits, but also for ASGM to take place over unexploited alluvial and colluvial deposits. Therefore, the total mining area increase from 2001 to 2012 is possibly a result of a combination of the increase in primary ore (industrial), and an increase in mining operations using water-jets systems on hillsides. The increase in ASGM area, associated with the new mining techniques, resulted in a TSS increase from about 30.0 to above 100.0 mg$\cdot L^{-1}$ in the Tocantins River, for example (Figure 10). The change in the Novo River was smaller, but high TSS values were also observed (~50.0 mg$\cdot L^{-1}$). In the Crepori River, the large extent of the mining area has had a direct impact on the TSS concentrations throughout the decades, however, the TSS concentrations in 2012 (~75.0 mg$\cdot L^{-1}$) were not as high as in 1993 (>300.0 mg$\cdot L^{-1}$) (Figures 10 and 11). This can be attributed to a few factors: (i) reduced numbers of miners (*garimpeiros*), and thus fewer active mining sites (*garimpos*); (ii) presence of medium-sized mining companies that have more control over their tailings, thus avoiding high sediment/tailing release into the waters; and (iii) reduced numbers of rafts along the tributaries in 2012, which are currently prohibited [4,5].

5.3. Management Recommendations and Future Research

One of the most important roles that temporal series of Landsat and IRS/LISSIII archive database plays is in the recovery of information concerning the temporal and spatial anthropogenic activities to support research on the socio-environmental impacts. With regards to ASGM, the consequences of water siltation to the aquatic environment, more specifically, to underwater light field and phytoplankton production, have been evaluated by [41]. In short, strong light attenuation reduces euphotic zone from 6 m to, approximately, 1 m in non-impacted and impacted water bodies, which can potentially change the phytoplankton community and decrease the photic zone and, thus, primary production. As a consequence of light attenuation, water siltation can change the fish community as suggested by [42]. The information produced in this paper indicates which rivers are subject to higher ASGM intensities that require more attention and investments for water and landscape recovery. Moreover, knowing the spatial distribution of sediment plume and the location of ASGM allows IBAMA and ICMBio (National Environmental Agencies) to monitor and control illegal/informal ASGM in protected areas, for example. Providing quantitative TSS values is strong evidence for

improving monitoring/controlling efforts (making them more effective), and indicative of a need to change techniques as suggested by [2], that reduces the mining tailings.

The introduction of high amounts of sediment can create an additional problem of erosion and deposition considering the projected five dams in the Tapajós River Basin. The creation of an artificial lentic (reservoir) environment combined with mining tailings can cause an impaired reservoir storage capacity [47] but can potentially create an optimum condition for algae bloom considering low water flow and increased nutrient input from mining tailings. This is without mentioning the potential mercury contamination that is carried out, adsorbed by the fine particles [38,48–50].

Similar analytical frameworks incorporating historical satellite imagery, geophysical characteristics, and optical data can be applied to other mined areas of the world, for example, in the French-Guiana, Suriname, Roraima and Mato Grosso in Brazil. Future research on modelling the sediment transport in pristine and mined sub-basins will be performed in order to investigate the contribution of mining tailing to total sediment transportation and support local and regional policies for a balanced environment.

6. Conclusions

Despite the severe consequences for the aquatic system, the quantification of mining-related areas in the Amazon and its consequential changes to water quality using satellite images is rarely performed. This is either due to a lack of water quality data (for example, TSS and Chlorophyll-a); or because of limitation of satellite images specifications such as spatial resolution (small rivers require spatial resolutions of about 5 m to be properly studied) [2,9,15].

This research paper presents an innovative remote sensing approach that combines land-use change and water quality information in order to investigate whether ASGM area extension is associated with water siltation. With the benefit of a 40-year period of the multi-satellite imagery archive, the use of DDV as a reference target to inter-calibrate the historical images was satisfactorily applied and presented reliable outputs to perform a multi-temporal analysis on land use and water siltation changes. In the case of the Tapajós River, the tributaries and the main channel are wide enough to be detected by medium-resolution satellite images such as Landsat (30 m) and IRS/LISSIII (24 m), and historical TSS were retrieved by [12].

The identification and quantification of ASGM in four sub-basins started with an official land use classification (TerraClass 2012) as a starting point. This classification, however, failed in identifying small ASGM polygons and a high misclassification rate was observed when validated with photos. Alternatively, Terraclass 2012 classification was updated with the support of auxiliary data and precise vector editing and used as baseline for a reverse in time classification of ASGM in 2001, 1993, 1984, and 1973. This procedure relies on the assumption that ASGM changes in the land cover are severe and remain detectable from satellite sensors for decades as demonstrated in this research.

In terms of the ASGM expansion and water siltation impacts, we observed that from 1973 to 1993, as mining areas increased, so did TSS concentrations for all sub-basins with significant ASGM. However, for the following decades, this association also depends on several other factors regarding ASGM activities, such as the applied mining technique (pans, drafts, water-jets, industrial methods), type of exploited gold deposits (alluvial, colluvial, quartz veins deposits), and intensity of gold mining, represented by the number of miners and gold production. The combination of these factors allows for the identification of four main chronological periods of change in the water quality of the studied rivers. Direct impacts of ASGM on the water quality is more evident during the first two decades (up to 1993) when the natural system was more susceptible. In the following decades, even with the increment of ASGM, the impact on the water is less evident because most of the new ASGM exploitation occurs further from the river network, and in which direct impacts are less perceptive. The period from 2004 to the present day is characterized by a major intensification of ASGM encouraged by high gold prices, with the presence of mining companies (industrial mining) exploiting primary deposits. The impact of this recent gold rush on water quality is evident, mainly in the Tocantins and Novo tributaries,

which raises awareness of the need for implementation of better mining techniques for water quality control and strict law enforcement in the present and near future.

Acknowledgments: This research was developed in a partnership among the University of Victoria (UVic), the Brazilian Institute for Space Research (INPE), and the Artisanal Gold Council. The authors would like to acknowledge logistical support by ICMBio (Brazilian Agency of Protected Areas). We also acknowledge financial support from the National Sciences and Engineering Research Council of Canada (NSERC) to Maycira Costa and NSERC Discovery Grant to Kevin Telmer. The São Paulo Research Foundation (FAPESP) grants to Evlyn Novo for field activities (Process n. 2011/23594-8 and 2008/07537-1). The CNPq (National Counsel of Technological and Scientific Development) awarded the lead author with a PhD scholarship (CNPq- Science without Borders n. 237930/2012-9), followed by a Post-Doctoral position (CNPq-PDJ n. 150835/2015-9) at INPE/Brazil.

Author Contributions: This research is part of *Felipe de Lucia Lobo*'s PhD Thesis defended in July 2015. He participated in every step of this article from planning, data collection, analysis and writing the manuscript as the first author. *Maycira Costa* was the main supervisor of this research and had an active participation in planning, data analysis, and text editing. *Evlyn Márcia Leão de Moraes Novo* was the co-supervisor of this research and was fundamental in defining the research approach and data analysis. *Kevin Telmer* is the Executive Director of the Artisanal Gold Council and provided key information for data analysis and discussion of the results.

Conflicts of Interest: The authors declare no conflict of interest, and no copyright issues with the data sources and documents cited.

Abbreviations

AERONET	Aerosol robotic network
AOT	Aerosol Optical Thickness
ASGM	Artisanal and Small-scale Gold Mining
DDV	Dense dark Vegetation
DN	Digital Number
FLAASH	Fast Line-of-sight Atmospheric Analysis of Hypercubes
IRS/LISSIII	Indian Remote Sensing/Linear Imaging Self Scanning Sensor
NIR	Near-Infrared
RGB	Red, Green, Blue
TOA	Top-of-Atmosphere
TSS	Total Suspended Solids

References

1. Veiga, M.M. *Mercury in Artisanal Gold Mining in Latin America: Facts, Fantasies and Solutions*; UNIDO: Vienna, Austria, 1997.
2. Sousa, R.N.; Veiga, M.M. Using performance indicators to evaluate an environmental education program in artisanal gold mining communities in the Brazilian amazon. *Ambio* **2009**, *38*, 40–46. [CrossRef] [PubMed]
3. Telmer, K.; Stapper, D. *Evaluating and Monitoring Small Scale Gold Mining and Mercury Use: Building a Knowledge-Base with Satellite Imagery and Field Work*; United Nations Industrial Development Organization: Victoria, BC, Canada, 2007.
4. Silva, A.R. *A Indústria Mineral no Pará*; Alberto Rogério Benedito da Silva: Belém, Pará, Brazil, 2012.
5. Fernandes, F.R.C.; Alamino, R.D.C.J.; Araújo, E.R. *Recursos Minerais E Comunidade: Impactos Humanos, Socioambientais E Econômicos*; CETEM/MCTI: Rio de Janeiro, Brazil, 2014.
6. CPRM. Província Mineral do Tapajós: Geologia, Metalogenia E Mapa Previsional Para Ouro Em SIG. Available online: http://www.cprm.gov.br (accessed on 15 April 2013).
7. Araújo Neto, H. *Perfil do Ouro*; Ministério de Minas e Energia: Brasília, Brazil, 2009.
8. Rodrigues, R.M.; Mascarenhas, A.F.S.; Ichihara, A.H.; Souza, T.M.C. *Estudo Dos Impactos Ambientais Decorrentes do Extrativismo Mineral E Poluição Mercurial no TAPAJÓS—Pré-Diagnóstico*; CETEM/CNPq: Rio de Janeiro, Brazil, 1994.
9. Roland, F.; Esteves, F.D. Effects of bauxite tailing on PAR attenuation in an amazonian crystalline water lake. *Hydrobiologia* **1998**, *377*, 1–7. [CrossRef]
10. Tudesque, L.; Grenouillet, G.; Gevrey, M.; Khazraie, K.; Brosse, S. Influence of small-scale gold mining on french guiana streams: Are diatom assemblages valid disturbance sensors? *Ecol. Indic.* **2012**, *14*, 100–106. [CrossRef]

11. Mol, J.H.; Ouboter, P.E. Downstream effects of erosion from small-scale gold mining on the instream habitat and fish community of a small neotropical rainforest stream. *Conserv. Biol.* **2004**, *18*, 201–214. [CrossRef]
12. Lobo, F.L.; Costa, M.P.F.; Novo, E.M. Time-series analysis of landsat-MSS/TM/OLI images over Amazonian waters impacted by gold mining activities. *Remote Sens. Environ.* **2015**, *157*, 170–184. [CrossRef]
13. Moran, M.S.; Bryant, R.; Thome, K.; Ni, W.; Nouvellon, Y.; Gonzalez-Dugo, M.P.; Qi, J.; Clarke, T.R. A refined empirical line approach for reflectance factor retrieval from landsat-5 TM and landsat-7 ETM+. *Remote Sens. Environ.* **2001**, *78*, 71–82. [CrossRef]
14. Hadjimitsis, D.G.; Clayton, C. Assessment of temporal variations of water quality in inland water bodies using atmospheric corrected satellite remotely sensed image data. *Environ. Monit. Assess.* **2009**, *159*, 281–292. [CrossRef] [PubMed]
15. Nery, M.A.C.; Silva, E.A.D. *Balanço Mineral Brasileiro: Ouro*; DNPM (Departamento Mineral de Produção Mineral): Brasília, Brazil, 2002.
16. ICMBIO. *Plano de Manejo-Floresta Nacional do Crepori-State of Pará*; Resumo Executivo: Curitiba, Brazil, 2010.
17. DGI/INPE. Divisão de Geração de Imagens. Available online: www.dgi.inpe.br (accessed on 1 May 2013).
18. MMA. Geographical Data: I3geo. Available online: http://mapas.mma.gov.br/i3geo/datadownload.htm (accessed on 2 March 2013).
19. SiBCS. *Sistema Brasileiro de Classificação de Solos*; Embrapa Solos: Rio de Janeiro, Brazil, 2006.
20. CPRM. Geobank. 2012. Available online: http://geobank.cprm.gov.br (accessed on 15 March 2013).
21. Coutinho, A.C.; Almeida, C.; Venturieri, A.; Esquerdo, J.C.D.M.; Silva, M. *Uso e Cobertura da Terra nas Áreas Desflorestadas da Amazônia Legal: Terraclass 2008*; EMBRAPA: Brasília, Brazil, 2013.
22. INPE. Topodata: Banco de Dados Geomorfométricos do Brasil. Available online: http://www.dsr.inpe.br/topodata (accessed on 13 March 2013).
23. Di Gregorio, A.; Jansen, L.J.M. Land Cover Classification System (LCCS). *Classification Concepts and User Manual for Software Version 1.0*; FAO/UNEP: Rome, Italy, 2000.
24. Shimabukuro, Y.E.; Smith, J.A. The least-squares mixing models to generate fraction images derived from remote sensing multispectral data. *IEEE Trans. Geosci. Remote Sens.* **1991**, *29*, 16–20. [CrossRef]
25. Chander, G.; Markham, B.L.; Helder, D.L. Summary of current radiometric calibration coefficients for landsat MSS, TM, ETM+, and EO-1 ALI sensors. *Remote Sens. Environ.* **2009**, *113*, 893–903. [CrossRef]
26. NASA/GSFC. Aerosol Robotic Network (Aeronet). Available online: http://aeronet.gsfc.nasa.gov (accessed on 13 March 2013).
27. Lu, D.; Mausel, P.; Brondizio, E.; Moran, E. Assessment of atmospheric correction methods for landsat TM data applicable to amazon basin lba research. *Int. J. Remote Sens.* **2002**, *23*, 2651–2671. [CrossRef]
28. Lu, D.; Mausel, P.; Brondízio, E.; Moran, E. Relationships between forest stand parameters and landsat TM spectral responses in the Brazilian Amazon basin. *For. Ecol. Manag.* **2004**, *198*, 149–167. [CrossRef]
29. Bezerra, O.; Veríssimo, A.; Uhl, C. *Impactos da Garimpagem de Ouro na Amazônia Oriental*; Imazon: Belém/PA, Portuguesa, 1998.
30. Villas Bôas, R.C.; Beinhoff, C.; Silva, A.R. *Mercury in Tapajos Basin*; CNPq/CYTED: Rio de Janeiro, Brazil, 2001.
31. Fearnside, P.M. Brazil's Cuiabá-Santarém (BR-163) Highway: The environmental cost of paving a soybean corridor through the Amazon. *Environ. Manag.* **2007**, *39*, 601–614. [CrossRef] [PubMed]
32. WRB/FAO. *World Reference Base for Soil Resources*, 1st ed.; International Soil Reference and Information Centre, ISRIC: Rome, Italy, 1998.
33. Junk, W.J.; Piedade, M.T.F.; Schöngart, J.; Cohn-Haft, M.; Adeney, J.M.; Wittmann, F. A classification of major naturally-occurring amazonian lowland wetlands. *Wetlands* **2011**, *31*, 623–640. [CrossRef]
34. DNPM. Sumário Mineral, 32. Available online: http://www.dnpm.gov.br (accessed on 5 April 2013).
35. Browder, J.O. Public policy and deforestation in the Brazilian Amazon. In *Public Policy and the Misuse of Forest Resources*; Gillis, R.R.A.M., Ed.; Cambridge University Press: Cambridge, UK, 1988; pp. 247–298.
36. Fearnside, P.M. Environmental destruction in the Brazilian Amazon. In *The Future of Amazonia: Destruction or Sustainable Development*; The Future of Amazonia: Macmillan, London, UK, 1990; pp. 179–225.
37. Junk, W. General aspects of floodplain ecology with special reference to amazonian floodplains. In *The Central Amazon Floodplain*; Junk, W., Ed.; Springer: Berlin/Heidelberg, Germany, 1997; Volume 126, pp. 3–20.
38. Telmer, K.; Costa, M.; Simões Angélica, R.; Araujo, E.S.; Maurice, Y. The source and fate of sediment and mercury in the Tapajós river, Pará, Brazilian Amazon: Ground- and space-based evidence. *J. Environ. Manag.* **2006**, *81*, 101–113. [CrossRef] [PubMed]

39. Almeida, R.; Shimabukuro, Y.E. Digital processing of a landsat-tm time series for mapping and monitoring degraded areas caused by independent gold miners, Roraima State, Brazilian Amazon. *Remote Sens. Environ.* **2002**, *79*, 42–50. [CrossRef]
40. Finer, M.; Novoa, S. Gold Mining Deforestation Continues to Expand in la Pampa (Madre de Dios, Peru). Available online: http://maaproject.org/2015/03/gold-mining-deforestation-expand-peruvian-amazon/ (accessed on 26 January 2016).
41. Lobo, F.; Costa, M.P.F.; Novo, E.M.; Telmer, K.H. Effects of artisanal small-scale gold mining tailings on the underwater light field in the Tapajós River basin. *Limnol. Oceanogr.* **2016**, in preparation.
42. Alho, C.R.; Reis, R.; Aquino, P.U. Amazonian freshwater habitats experiencing environmental and socioeconomic threats affecting subsistence fisheries. *Ambio* **2015**, *44*, 412–425. [CrossRef] [PubMed]
43. Biggs, T.W.; Dunne, T.; Martinelli, L.A. Natural controls and human impacts on stream nutrient concentrations in a deforested region of the Brazilian amazon basin. *Biogeochemistry* **2004**, *68*, 227–257. [CrossRef]
44. Deegan, L.A.; Neill, C.; Haupert, C.L.; Ballester, M.V.R.; Krusche, A.V.; Victoria, R.L.; Thomas, S.M.; Moor, E. Amazon deforestation alters small stream structure, nitrogen biogeochemistry and connectivity to larger rivers. *Biogeochemistry* **2010**, *105*, 53–74. [CrossRef]
45. Farella, N.; Lucotte, M.; Louchouarn, P.; Roulet, M. Deforestation modifying terrestrial organic transport in the rio tapajós, Brazilian amazon. *Org. Geochem.* **2001**, *32*, 1443–1458. [CrossRef]
46. Telmer, K.H. The Effect of Changing Gold Prices on Artisanal Mining. Available online: http://artisanalgold.blogspot.ca (accessed on 2 April 2015).
47. Shalash, S. Effects of sedimentation on the storage capacity of the high aswan dam reservoir. *Hydrobiologia* **1982**, *91*, 623–639. [CrossRef]
48. Boudou, A.; Maury-Brachet, R.; Coquery, M.; Durrieu, G.; Cossa, D. Synergic effect of gold mining and damming on mercury contamination in fish. *Environ. Sci. Technol.* **2005**, *39*, 2448–2454. [CrossRef] [PubMed]
49. Park, J.-G.; Curtis, R.L. Mercury distribution in sediments and bioaccumulation by fish in two oregon reservoirs: Point-source and nonpoint-source impacted systems. *Arch. Environ. Contam. Toxicol.* **1997**, *33*, 423–429. [CrossRef] [PubMed]
50. Egler, S.G.; Rodrigues-Filho, S.; Villas-Bôas, R.C.; Beinhoff, C. Evaluation of mercury pollution in cultivated and wild plants from two small communities of the Tapajós Gold Mining Reserve, Pará State, Brazil. *Sci. Total Environ.* **2006**, *368*, 424–433. [CrossRef] [PubMed]